Chemical Geology 466 (2017) 491–499

Contents lists available at ScienceDirect

Chemical Geology

journal homepage: www.elsevier.com/locate/chemgeo

Garnet growth after overstepping

Frank S. Spear

Department of Earth and Environmental Sciences, Rensselaer Polytechnic Institute, 110 8th Street, Troy, NY 12180, USA

ARTICLE INFO

Keywords:
Garnet
Nucleation
Growth
Overstepping
Affinity
Zoning

ABSTRACT

Overstepping of metamorphic reactions is required to provide the driving force necessary for porphyroblast nucleation and growth. Forward models of garnet nucleation and growth are presented assuming an affinity for nucleation that corresponds to several tens of degrees or several kilobars of overstepping. The composition of garnet that nucleates and grows is assumed to be that which provides the largest decrease in free energy. With these assumptions, the zoning predicted for a garnet grown under isothermal, isobaric conditions is revealed to be sufficiently similar to the zoning predicted for garnet grown under continuous near-equilibrium conditions that distinction based on the shape of zoning profiles alone does not appear to be possible. Furthermore, the growth of an initial garnet crystal following nucleation after overstepping depletes the affinity for subsequent nucleation by sequestration of Mn into the existing garnet crystal. Progressive nucleation, therefore, requires additional energy input, most likely through changes in pressure and temperature, to replenish the affinity. The predicted zoning in garnets nucleated following substantial growth of the first nucleated garnet does not match the typical bell-shaped profile of Rayleigh fraction but rather displays distinctly diagnostic zoning depending on the assumed rate limiting step for growth. Diffusion controlled growth results in relatively broader and flattened profiles whereas interface controlled growth results in later garnets having a peaked core Mn profile. This latter profile would relax by diffusion in relatively short times (less than 1 Ma) and would thus not likely to be preserved, but appears to have been observed in garnet zone samples from central Vermont. Calculations for this sample also indicate that garnet ceased growing when chlorite was exhausted, at which point considerable affinity remained indicating that equilibrium was not achieved. Tectonic interpretations based on P–T paths calculated assuming near-equilibrium nucleation and growth of garnet are thus likely to require reevaluation in light of the magnitude of overstepping needed for nucleation and the possibility that equilibrium was not attained at the metamorphic peak.

1. Introduction

A number of recent papers have concluded that equilibrium isograd reactions may be overstepped by a considerable amount before nucleation of a new porphyroblast occurs (e.g. Waters and Lovegrove, 2002; Wilbur and Ague, 2006; Pattison and Tinkham, 2009; Pattison et al., 2011; Spear et al., 2014). Values of affinity estimated for the nucleation of garnet range from 166 to 2200 J/mol oxygen, representing overstepping of up to 80° or 4–5 kbar (Waters and Lovegrove, 2002; Wilbur and Ague, 2006; Pattison et al., 2011; Spear et al., 2014; Castro and Spear, 2016). Implications for the interpretation of pseudosections in light of this degree of overstepping are discussed in Spear and Pattison (2017).

If a porphyroblast such as garnet does not nucleate until there has been enough overstepping to build these levels of affinity, then it cannot have grown continuously at near-equilibrium conditions as it traverses along the rock's P–T path. Rather, the above studies suggest that, once nucleated, garnet may grow at near isobaric-isothermal conditions (e.g. Hollister, 1969; Spear et al., 2014). If so, the chemical zoning recorded by the garnet cannot reflect a succession of near-equilibrium growth stages, as has been so commonly assumed (e.g. Spear and Selverstone, 1983; Gaidies et al., 2008). This in turn calls to question the practice of using the chemical zoning in garnet to infer the P–T path based on the assumption of near-equilibrium.

The question arises: if garnet nucleates at conditions considerably above the equilibrium isograd reaction, then what controls the chemical zoning of the garnet? Hollister (1966) attributed the zoning of Mn in garnet from the Kwoiek area, British Columbia to Rayleigh fractionation, a process by which the growing garnet sequesters Mn (and other elements) as it grows, depleting the reservoir from which garnet is growing in this component. In addition, Hollister (1966) demonstrated that the classic bell-shaped zoning profiles commonly exhibited by Mn in garnet could be achieved by an isothermal, isobaric process (i.e. Rayleigh fractionation with a constant partition coefficient). Whereas

E-mail address: spearf@rpi.edu.

http://dx.doi.org/10.1016/j.chemgeo.2017.06.038
Received 2 March 2017; Received in revised form 26 June 2017; Accepted 28 June 2017
Available online 03 July 2017

Rayleigh fractionation undoubtedly plays a major role in the development of Mn zoning, it is essentially an equilibrium fractionation between the garnet and the reservoir. It is still necessary to maintain a driving force for growth (i.e. affinity).

Subsequent investigations employed more comprehensive sets of equilibrium relations between garnet and matrix phases and arrived at essentially the same conclusions as Hollister (1966) (e.g. Spear et al., 1990; Symmes and Ferry, 1992). Significantly, these latter models assumed a continuum of near-equilibrium conditions along a P–T path to achieve representative garnet zoning, with no role for Rayleigh processes at constant temperature and pressure such as proposed by Hollister (1966). Frost and Tracy (1991) examined this topic and concluded that observed Ca zoning in garnet could be achieved by isothermal, isobaric processes through Rayleigh fractionation.

The purpose of the present communication is to present the theoretical framework within which the chemical zoning of garnet can be calculated following nucleation after considerable overstepping. Model zoning profiles will be presented for a rock containing a single or multiple garnets, and compared to model zoning profiles assuming equilibrium. Criteria for identifying a garnet that has grown out of equilibrium from its zoning pattern will be discussed. Finally, the question of whether equilibrium is ever achieved in a rock undergoing metamorphism will be addressed.

2. Theory

Affinity is the energy available to drive nucleation or chemical reaction and may be defined as either the partial derivative of Gibbs energy with reaction progress at constant temperature and pressure:

$$A = -\left(\frac{\partial G}{\partial \xi}\right)_{P,T}$$

or the change in Gibbs energy in going from reactants to products of a chemical reaction ($-\Delta G$). The second definition is most appropriate for the consideration of nucleation as was utilized by Spear and Pattison (2017) and the first definition is most appropriate for consideration of garnet growth under isothermal, isobaric conditions, as discussed here.

Following Gaidies et al. (2011), Pattison et al. (2011) and Spear et al. (2014), the affinity for nucleation of a porphyroblast such as garnet may be calculated as the difference between the G of the nucleated garnet and the fictive G of a compound of the same composition as the nucleated garnet calculated from the chemical potentials of the garnet-free matrix phases (Fig. 1a). Inasmuch as Gibbs free energy (G) changes with pressure and temperature, the affinity available for nucleation will also vary with P and T as a function of the ΔV and ΔS of reaction, respectively. The G of garnet is a function of composition so the affinity for nucleation is also a function of the garnet composition. Following the treatment in Thompson and Spaepen (1983) it was assumed by the above authors that the most likely composition of garnet to nucleate would be that with the greatest affinity (Fig. 1a), the reason being that this composition generates the most available energy to overcome the activation energy barrier for nucleation (see also discussion in Spear and Pattison, 2017).

Following nucleation out of equilibrium, garnet will grow such that the compositions of the garnet and matrix phases evolve along their respective free energy surfaces until eventually equilibrium is closely attained (Fig. 1b, c). It is proposed that the composition of garnet formed during this continuous evolution is also that which provides the largest change in free energy: that is, the same criteria used to ascertain the composition of garnet that would form upon nucleation. Although the affinity required to drive the continuous reaction is most likely considerably smaller than the affinity required for nucleation, growth of garnet in steps that maximizes the decrease in free energy at each increment is consistent with the general trend of the system towards minimizing G. Furthermore, maintaining this assumption results in a continuum of compositional changes. This assumption also requires that the garnet is completely unreactive, such that every growth step is essentially the same as nucleating a new garnet, which is assumed to grow on the old garnet.

It is also implicit that the *composition* of garnet is not controlled by kinetic factors (e.g. rates and mechanisms of dissolution/precipitation at mineral surfaces, or of intergranular transport of nutrients), and that the composition is rather being only determined by this maximum free energy decrease. The validity of this assumption requires that the availability of Mg, Fe, Mn and Ca is not limited at the growing garnet interface. Additionally, the *rate* of garnet growth must be controlled by kinetic factors such as diffusion of Si or Al or surface attachment or detachment kinetics, otherwise, once nucleated, the garnet would grow instantaneously. In other words, the diffusivities of Mg, Fe, Mn and Ca are assumed to be rapid relative to the rate of garnet growth.

Calculating the composition of garnet requires finding the garnet composition such that the tangent to the garnet G surface is parallel to the tangent defined by the matrix phases. The equations needed to calculate this most likely garnet composition are as follows. Equations that constrain the slope of the tangent to the garnet G surface ($\mu_i^{Grt} - \mu_j^{Grt}$) are, according to the above assumptions, equal to those that constrain the slope of tangent to the matrix assemblage ($\mu_i^{Matrix} - \mu_j^{Matrix}$). There are three such independent equations:

$$\begin{aligned}
\mu_{alm}^{Grt} - \mu_{prp}^{Grt} &= \mu_{alm}^{Matrix} - \mu_{prp}^{Matrix} \\
\mu_{sps}^{Grt} - \mu_{prp}^{Grt} &= \mu_{sps}^{Matrix} - \mu_{prp}^{Matrix} \\
\mu_{grs}^{Grt} - \mu_{prp}^{Grt} &= \mu_{grs}^{Matrix} - \mu_{prp}^{Matrix}
\end{aligned} \quad (1)$$

The chemical potentials of the garnet components in the matrix assemblage are calculated as linear combinations of matrix phase components, for example:

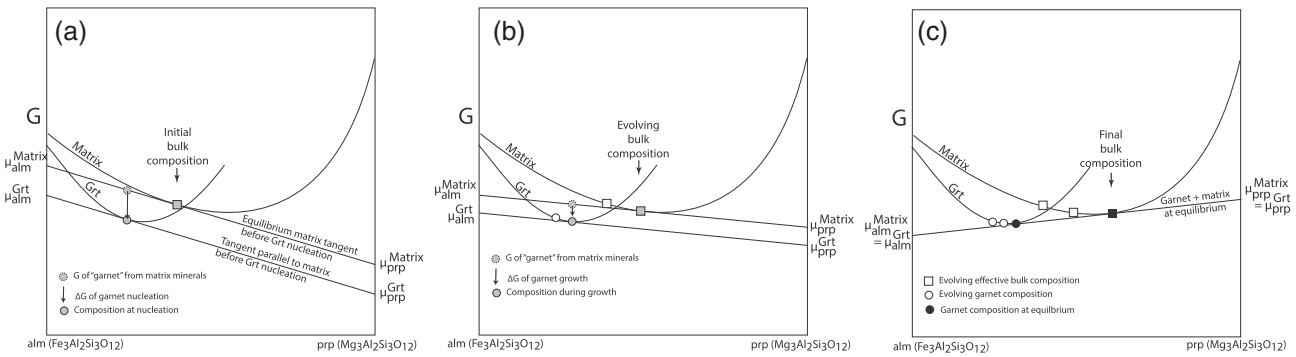

Fig. 1. Schematic G-X diagrams for matrix + garnet showing the evolution of garnet and matrix compositions during garnet growth following overstepping. (a) Configuration at garnet nucleation. (b) Configuration during growth. (c) Configuration at equilibrium. The composition of garnet is that which provides the maximum decrease in free energy (arrow in (a) and (b)). Note that the figure assumes complete equilibrium among the matrix phases.

$$\mu_{prp}^{Matrix} = 1.333\mu_{qtz}^{Qtz} + 0.333\mu_{clinochlore}^{Chlorite} + 0.333\mu_{amesite}^{Chlorite} - 2.667\mu_{H_2O}^{Matrix} \quad (2)$$

The chemical potentials of the matrix assemblage are known from solution of the equilibrium relations for these phases at the specified pressure, temperature and bulk composition. The only unknowns are therefore the three independent components of garnet, which are solved by Newton's method using Eq. (1). The difference in energy available for reaction is then calculated as:

$$\mu_{prp}^{Grt} - \mu_{prp}^{Matrix} = \mu_{alm}^{Grt} - \mu_{alm}^{Matrix} = \mu_{sps}^{Grt} - \mu_{sps}^{Matrix} = \mu_{grs}^{Grt} - \mu_{grs}^{Matrix} \quad (3)$$

This value is exactly equivalent to the first definition of affinity given above. Note that the value affinity is only valid at the specific P, T and extent of reaction of the calculations and will with reaction progress as the system approaches equilibrium. All thermodynamic calculations were done in the MnNCKFMASH system using code written for Program Gibbs with thermodynamic data from Spear and Pyle (2010).

Forward modeling was achieved by picking an arbitrary P and T above the equilibrium garnet isograd reaction and performing successive calculations of the garnet composition. The bulk composition used in these calculations is that of a typical pelitic schist (Table 1). After each iteration, the bulk composition is modified by subtracting the garnet that was produced and the compositions of all other phases adjusted according to their equilibrium conditions. Because the rate limiting mechanism for garnet growth is not known, an arbitrarily small quantity of 10^{-5} mol was "grown" and subtracted from the bulk composition on each iteration.

A goal of this modeling was to compare the overstepped garnet zoning profile (the "OS" model) with the zoning profile that would be produced by progressive garnet growth at near equilibrium conditions (the "EQ" model). This type of equilibrium forward modeling requires a P–T path to be specified, and a path from 500 °C, 5 kbar to 700 °C, 10 kbar (25 bars/degree) was chosen. The P–T conditions for the OS calculations are 657 °C, 8.925 kbar, equivalent to the conditions along the P–T path where chlorite vanishes from the assemblage in the EQ model. This was chosen so that the final conditions of the EQ model would be the same as those of the OS model. Both the OS and EQ models incorporate Rayleigh fractionation. Note that both models only consider the reacting assemblage chlorite + biotite + muscovite + plagioclase + quartz and equilibria involving possible staurolite or kyanite were not considered.

3. Results

The results of the initial set of calculations are shown in Fig. 2. As can be seen, the general shape of the zoning is similar for both the OS and EQ models. In particular, the Mn content decreases from core to rim in the classic bell-shaped profile for both models, consistent with Rayleigh fractionation. The composition of the garnet core differs somewhat between the two models, which might be used to distinguish between overstepping and equilibrium growth, but only if the reactive bulk rock composition were precisely known. Ca is the only element that displays a different zoning trend in the OS versus EQ models, although the magnitude of the changes in grossular would make this difficult to distinguish. Note that the composition at the garnet rim is the same for both models, as it must be because both models were terminated at 657 °C, 8.925 kbar when it is assumed that equilibrium was achieved. It should also be noted that size of the garnets (around 7.2 mm) depends entirely on the size of the bulk composition modeled, in this case 100 g (approximately 37 cm^3).

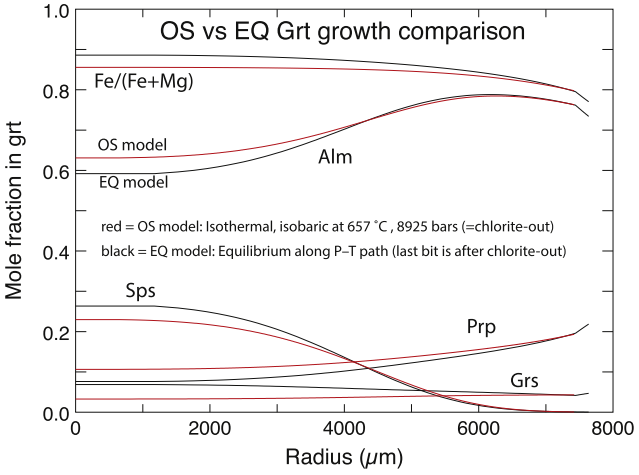

Fig. 2. Plot of modeled garnet composition versus radius for the OS and EQ models. Note that the small amount of additional garnet growth in the EQ model (black) beyond the OS model (red) occurs as a result of garnet growth after chlorite is exhausted. (For interpretation of the references to colour in this figure legend, the reader is referred to the web version of this article.)

The one zoning characteristic that does provide a suggestion of the difference between the OS and EQ models is Fe/(Fe + Mg). For equilibrium growth of garnet from chlorite, the Fe/(Fe + Mg) decreases monotonically with increasing temperature and is a good proxy for temperature because the value is not strongly pressure dependent. For the above example, the change in Fe/(Fe + Mg) for the EQ model is − 0.079 (0.886 to 0.807) over a temperature increase of 65°. In contrast, the change in Fe/(Fe + Mg) for the OS model is − 0.058 (0.856 to 0.798) under isothermal conditions. The reason the Fe/(Fe + Mg) changes at all in garnet grown isothermally is the modification of the bulk composition as garnet fractionates. Although the difference between the OS and EQ models is small, it might be used to infer garnet growth under non-equilibrium conditions. In summary however, there appears to be no single distinguishing characteristic in the chemical zoning that would make the OS model simple to recognize.

One aspect of the OS model not obvious in Fig. 2 is that as garnet grows and the bulk composition is modified by garnet fractionation, the available affinity decreases until eventually equilibrium is attained and the affinity is zero. At the point of nucleation, the affinity in the OS model calculations is around 812 J/mol oxygen and decreases non-linearly to zero after 1471 iterations. It is important to note that the modeling presented here assumes that the affinity required to drive the reactions responsible for garnet growth is less than that required for garnet nucleation, so the initial garnet can continue to grow even though the affinity is less than that required for nucleation of additional garnets.

Table 1
Bulk rock analyses used in calculations (weight % oxides).

	TM-549[a]	TM-626[b]	TM-626[c]
SiO_2	55.71	55.72	57.98
Al_2O_3	20.84	16.16	15.82
MgO	3.61	3.97	4.17
FeO	6.38	10.76	8.76
MnO	0.17	0.44	0.05
CaO	0.97	0.64	0.36
Na_2O	1.80	1.25	1.38
K_2O	5.81	4.05	4.49
H_2O[d]	4.72	6.0	7.0

[a] Composition determined from modal analysis of X-ray maps using ImageJ multiplied by phase composition.
[b] Composition determined from average electron microprobe spot analyses with broadened beam.
[c] Composition calculated by subtracting garnet from the whole rock bulk composition.
[d] Sufficient H_2O was added to each bulk composition to ensure excess fluid at all P-T conditions.

3.1. Progressive nucleation

The steady decrease in affinity as garnet fractionates in the OS model raises a significant question regarding the process of progressive nucleation. There are numerous studies that have concluded that nucleation of garnet is progressive, principally based on the observation that the Mn content of garnet cores correlates strongly with the size of the garnet, with smaller garnets being Mn-poorer (e.g. Chernoff and Carlson, 1997; Spear and Daniel, 1998, 2001; George and Gaidies, 2017). The assumption in the above studies and the present modeling is that the diffusion of Mn along grain boundaries is rapid so that the Mn content on the rims of all growing garnets is identical, whether based on EQ or OS modeling. Thus, the Mn content of garnet can serve as a proxy for time, leading to the conclusion that the smaller garnets nucleated later than the larger garnets. If the affinity decreases as the initial garnet grows, however, the driving force for subsequent nucleation will decrease below the nucleation threshold (e.g. 812 J/mol oxygen in the present study), thus prohibiting subsequent nucleation.

In order to replenish the affinity to provide the driving force for progressive nucleation, it is necessary for P and T to steadily increase following the nucleation of the initial garnet. This is essentially the assumption made by Kelly et al. (2013a, 2013b) in their modeling of garnet growth. The rate of affinity generation depends on the ΔS and ΔV of reaction, the specific P–T path, and the rate of change of P and T. Along the P–T path used in the above modeling calculations, the affinity increases at a rate of approximately 12.5 J for every 1° and 25 bars (Fig. 3a). For every millimole of garnet that is grown, the affinity decreases by around 117 J (Fig. 3b). An increase in P and T of around 10° would thus be required to replenish the affinity depletion from each millimole of garnet produced back to the threshold value for nucleation.

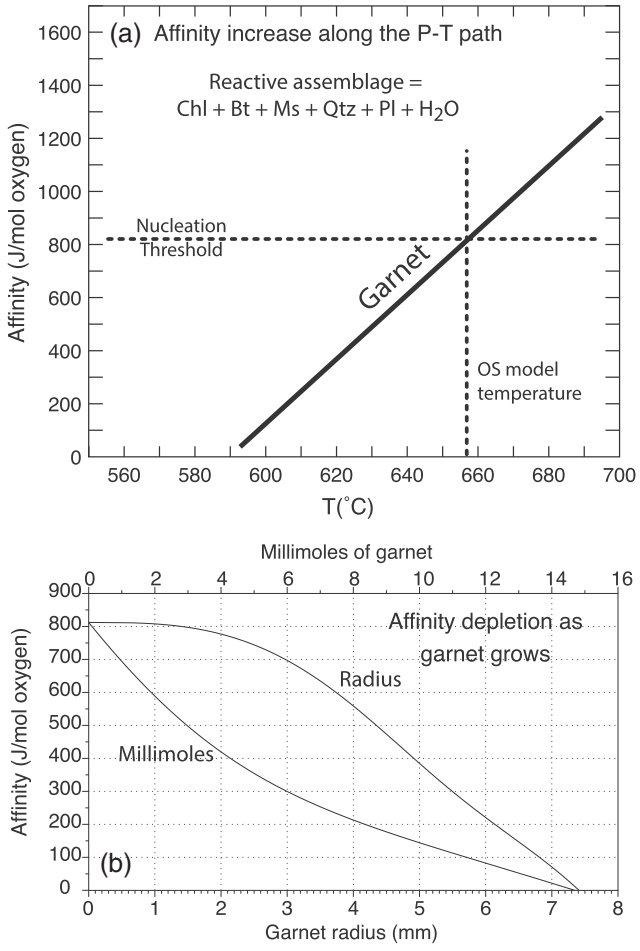

Fig. 3. (a) Plot of affinity generation versus temperature along the modeled P–T path. (b) Plot showing the decrease in affinity versus garnet growth (in units of millimoles and radius) as a result of the sequestering of Mn into the fractionating garnet core.

Assuming a constant threshold of affinity for nucleation, the rate of nucleation will depend on the interplay of two rates: the crystal growth rate (which determines the rate of affinity depletion) and the heating (or loading) rate (which determines the rate of affinity replenishment). Neither of these values is well known so rather than assume values for crystal growth rate and heating rate, the approach taken here is to introduce new garnet nuclei at arbitrarily specified Mn concentrations (e.g. X_{sps} = 25, 20, 15, 10, 5). Given that the goal of this section is calculation of the zoning profiles in a suite of progressively nucleated garnets, this approach is warranted, provided a model for the attachment of new garnet onto existing crystals can be formulated.

Kretz (1974) discussed three geometric possibilities for garnet growth and Spear and Daniel (1998) examined the consequences for zoning of these three models: the addition of new material in constant radial amounts, in amounts proportional to each crystal's surface area, and in equal mass amounts. Whereas there is no firm theoretical justification for the second and third geometric options, the addition of material in equal radial amounts may be attributed to isothermal interface-controlled growth (see Discussion below).

The rate of attachment of new material onto existing garnet crystals depends on the rate-limiting step for garnet growth. Continuing with the assumption of a rapid transport step, the rate of garnet growth that is limited by interface kinetics follows from the equations for the rate of attachment (on the garnet) and detachment (from the reactant phases):

$$r = \nu \exp(-\Delta G/RT) \quad (4)$$

where r is the rate of attachment or detachment, ν is the jump frequency, ΔG is the activation energy for attachment or detachment, R is the gas constant and T is temperature (e.g. Volmer and Marder, 1931; Kirkpatrick, 1975). Inasmuch as there is no radial dependence in this expression, the rate of attachment must be the same for all crystals (Fig. 4a).

In a related model, it is assumed that each growing crystal sequesters material from a spherical shell of equal radius around the existing crystal (Fig. 4a). The volume of the shell is, of course, larger for crystals of greater radius, but the incremental radius of the shell is identical for each. From Fig. 4a we have

$$\Delta r = r_2 - r_1$$

$$V_i = \tfrac{4}{3}\pi(r_2^3 - r_1^3) = \tfrac{4}{3}\pi((\Delta r + r_1)^3 - r_1^3)$$

$$V_i = \tfrac{4}{3}\pi(\Delta r^3 + 3\Delta r^2 r_1 + 3\Delta r r_1^2)$$

and

$$V_{total} = \sum V_i$$

Since mass is proportional to volume, the distribution of masses is proportional to the distribution of volumes of the shells:

$$m_i = m_{total}\frac{V_i}{V_{total}} \quad (5)$$

Once the incremental mass is calculated for either model, the radial change is then

$$r_2^3 = \left(\frac{3}{4\pi}\right) m_i \cdot (\text{molar volume}) + r_1^3$$

Note that this model gives exactly the same result as assuming equal radial increments on each crystal (Eq. (4)).

Garnet growth limited by diffusion of Al in the matrix has been proposed by Carlson (1989, 1991) (see also Denison and Carlson, 1997) and of Si by Spear and Daniel (2001). The distribution of new mass onto existing crystals where growth is diffusion-limited depends on the nature of the diffusive flux. If it is assumed that the diffusion is steady-

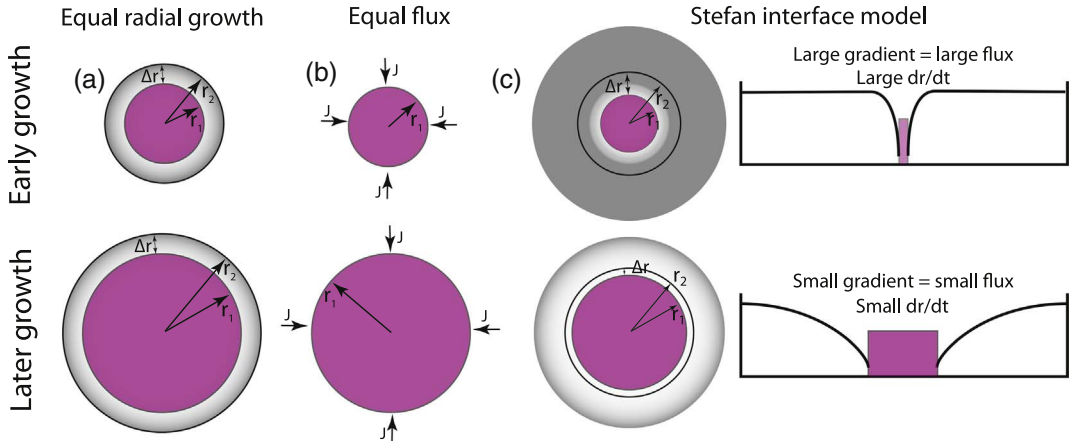

Fig. 4. Schematic representations of the three models for distributing mass onto crystals of different sizes. (a) Each crystal sequesters new mass from a spherical shell of radius Δr. (b) The flux to the surface of each crystal is equal. (c) Stefan interface model. Small crystals grow more rapidly than large crystals due to larger gradient at crystal interface.

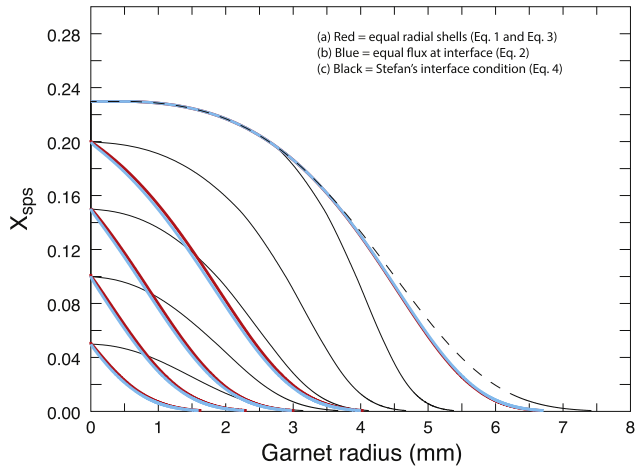

Fig. 5. Plot of X_{Sps} versus garnet radius for successively nucleated garnets in the OS model. Allocation of new mass based on the assumption of (a) equal radial increments; (b) constant flux to all growing garnet crystals; (c) Stefan's interface condition. Dashed line shows Mn zoning profile if only a single garnet nucleates within the model volume.

state, then the gradient surrounding each crystal is identical and the flux to each crystal surface (in units of mass/unit area) will be identical (Fig. 4b). The total mass added to each crystal is then equal to this flux times the surface area of the crystal. That is,

$$m_i = J 4\pi r_i^2$$

where J is the flux and m_i is the mass being added to crystal i. Inasmuch as

$$\sum m_i = m_{total}$$

we have

$$J = \frac{m_{total}}{4\pi \sum_{i=1}^{n} r_i^2}$$

so the mass added to each crystal is.

$$m_i = \frac{4\pi r_i^2 m_{total}}{4\pi \sum_{i=1}^{n} r_i^2} = \frac{r_i^2 m_{total}}{\sum_{i=1}^{n} r_i^2} \quad (6)$$

That is, the mass is distributed in proportion to the surface areas of the crystals (i.e. proportional to the squares the radii). Large crystals will get more mass and a slightly larger radial increase than small crystals.

A more rigorous treatment of the predicted mass allocation for

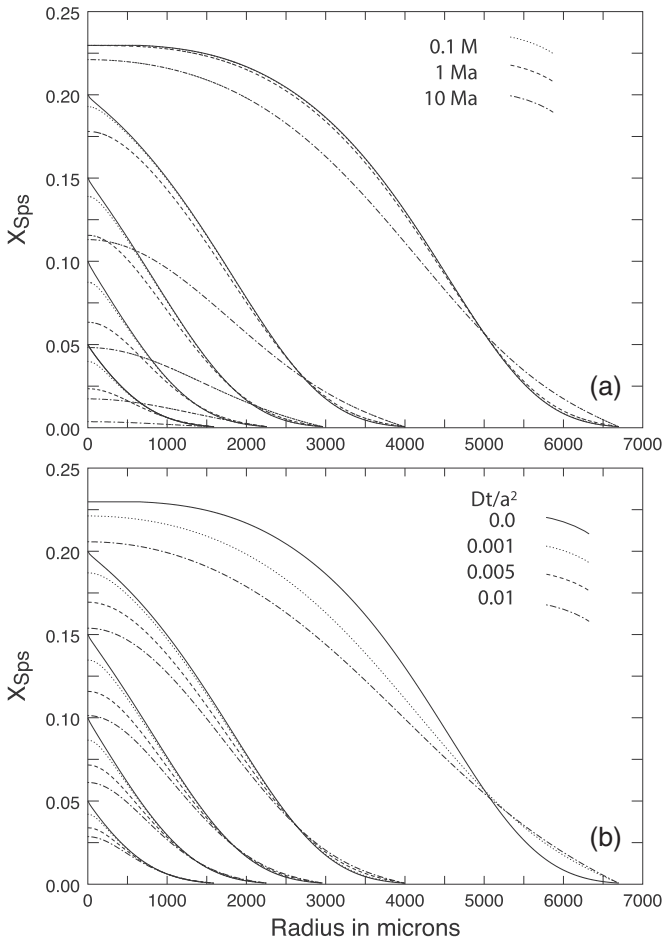

Fig. 6. (a) Plot of X_{Sps} versus garnet radius for the successively nucleated garnets from Fig. 5 after diffusional relaxation. Diffusion was calculated at 700 °C for total times of 0.1, 1, and 10 Ma. (b) Same plot as in (a) except profiles are drawn at constant values of dimensionless time (Dt/a^2).

diffusion-limited crystal growth recognizes that the diffusive halos surrounding growing crystals evolve with time (the non-steady state or time-dependent model; e.g., Glicksman, 2000). At short times for newly nucleated crystals, the gradient is steep and the flux to the crystal is large; as time progresses the gradient flattens and the flux decreases (Fig. 4c). Theoretical analysis begins with the mass balance that equates the rate of change of the volume of the crystal with the flux of material arriving at the interface, known as Stefan's interface condition.

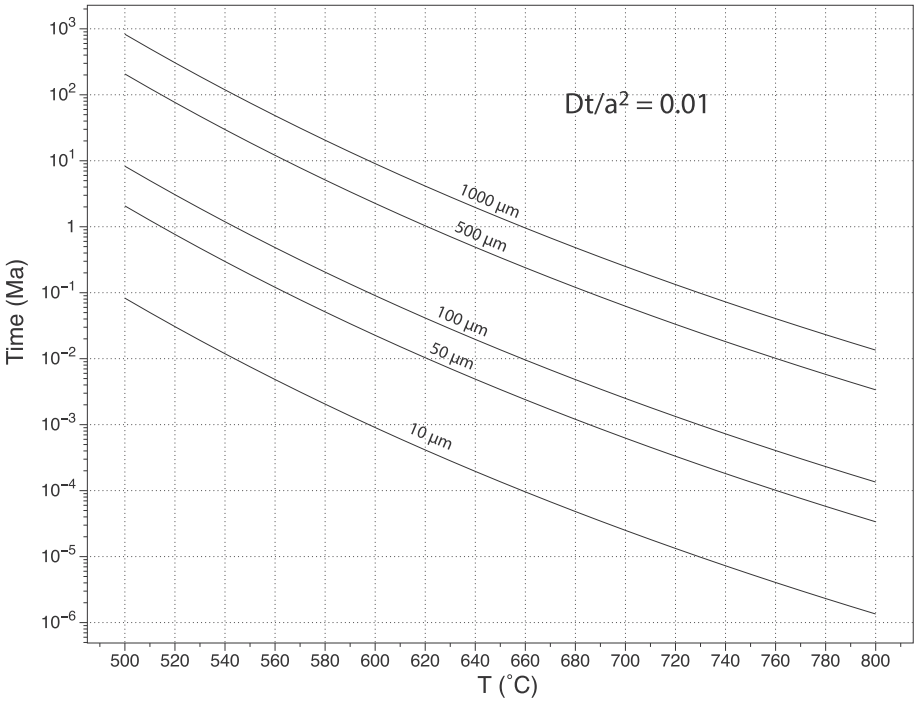

Fig. 7. Plot of log time versus T contoured for crystal radius at a value of dimensionless time (Dt/a^2) of 0.01.

Following the treatment in Glicksman (2000), we have for Stefan's interface condition:

$$4\pi r^2(C_{GB} - C_{Grt})\frac{dr}{dt} - 4\pi r^2 J = 0$$

At sufficiently long times the flux at the interface becomes steady state, although still dependent on the crystal size:

$$J = \frac{D(C_{GB} - C_{Matrix})}{r}$$

So

$$\frac{dr}{dt} = \frac{D}{r}\frac{(C_{GB} - C_{Matrix})}{(C_{GB} - C_{Grt})}$$

That is, the radial change in garnet in a given crystal is proportional to the inverse of the radius: small crystals increase their radius more rapidly than do large crystals. Because the change in volume is related to the change in radius:

$$\frac{dV}{dt} = 4\pi r^2\frac{dr}{dt}$$

and the change in mass is proportional to the change in volume (assuming a constant molar volume), we can write

$$m_i = m_{total}\frac{r_i}{\sum r_i} \quad (7)$$

from which we can calculate the radial growth of each garnet crystal as before.

In summary, both the distribution of mass to existing crystals for interface controlled growth (Eq. (4)) and growth based on sequestering material from equal spherical shells (Eq. (5)) predict equal radial increments (Fig. 4a), whereas constant surface flux (Eq. (6)) predicts large crystals grow slightly more than smaller crystals (Fig. 4b). Non steady state diffusion controlled growth (Eq. (7)) predicts small crystals grow more rapidly than large crystals (Fig. 4c).

The results of the progressive nucleation calculations are presented in Fig. 5. The dashed line shows the results for a single garnet in the sample volume and displays the bell-shaped profile typical of garnets from the garnet zone. The shape of X_{sps} zoning depends on the assumed model. For equal radial increments (Eq. (4)), equal shell volumes (Eq. (5)), and equal flux at the interface (Eq. (6)) the profiles of X_{sps} for all by the initial garnet show peaked X_{sps} profiles in the cores. In contrast, the profiles for the Stefan's interface condition (Eq. (7)) show broadened profiles in the cores. The X_{sps} profiles for the Stefan's interface model (solid black lines in Fig. 5) are also considerably shallower for the smaller garnets and considerably steeper for the largest (initial) garnet than is evident in the first two models (equal radial shells and equal flux).

The zoning profiles in Fig. 5 may be compared with observed zoning profiles of garnets of various sizes from natural samples. There have been a few studies in which a suite of garnets of differing sizes from a single rock have been cut through their centers, the most notable being that of Chernoff and Carlson (1997). Garnet crystals from that study display Mn zoning with well-defined rounded tops at their centers, which would suggest that the Stefan's interface model may pertain. However, the small garnets from that study also display steep shoulders with decreasing Mn content, in contradiction to the calculated zoning profiles for this model.

It is important to consider the effect of diffusional relaxation on the profiles presented in Fig. 5. To this end, numerical experiments were performed on the profiles for the equal radius model and the results are shown in Fig. 6. Each profile was used as the initial condition in an explicit finite difference diffusion model with spherical geometry using the Mn diffusion coefficient from Chakraborty and Ganguly (1992). The grid spacing was 2 μm and sufficiently small time steps were used to ensure numerical stability. The resulting profiles were saved after specified increments of absolute and dimensionless time (Dt/a^2). It is clear from the plots shown in Fig. 6 that even a modest amount of diffusion will sufficiently relax the profiles to cause the peak in the garnet core to disappear. Spherical diffusion affects the garnet core more than the rim so that, even after moderate diffusion has occurred, the profiles are not so flat as those of the Stefan's interface model.

The magnitude of diffusional relaxation scales with the diffusivity (and thus with the temperature), the length scale, and the time. The crystals in Figs. 5 and 6 are relatively large (1.6 to 6.7 mm radius). Garnets from typical Barrovian garnet zones are usually smaller (typically 1–3 mm) and smaller garnets will relax more quickly than larger garnets at the same conditions. Fig. 7 is a plot of log time versus temperature contoured for values of garnet radius for a value of Dt/

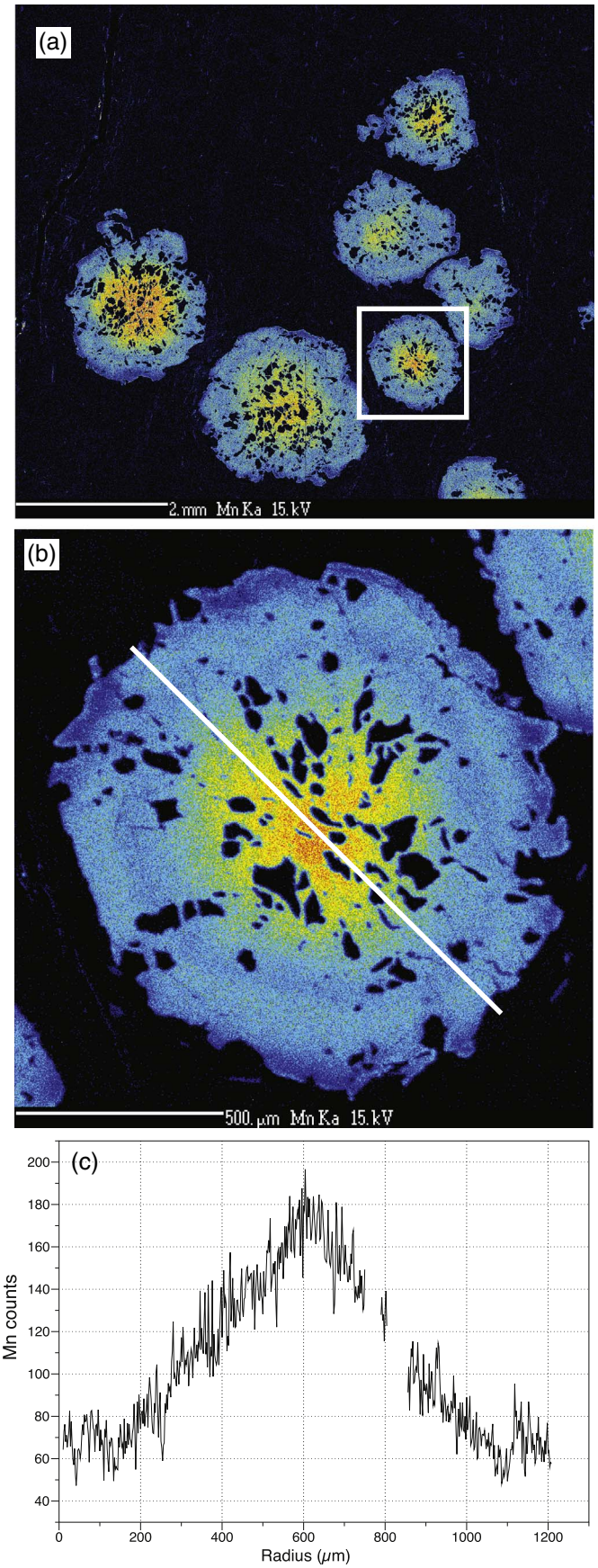

Fig. 8. Mn zoning in sample TM-918c from central Vermont, USA. (a) X-ray map showing Mn zoning in several garnets. Box shows the location of garnet in (b). (b) Close up of an individual garnet. Line shows the location of profile in (c). (c) Profile (Mn versus radius) of Mn zoning through the garnet core. Blank areas are quartz inclusions.

a^2 = 0.01. The time scale for diffusional relaxation of the core to the degree shown by the dot-dashed lines in Fig. 6b (Dt/a^2 = 0.01) for any sized crystal can be read from the plot. For example, a 100 µm radius garnet crystal would experience diffusional relaxation equivalent to Dt/a^2 = 0.01 in 0.1 Ma. Thus, it is not likely that the central core peak would ever be preserved in natural samples unless growth and subsequent cooling was quite rapid. Moreover, it is worth noting that the central core peak Mn profiles should only be observed in smaller, later nucleated garnets. In many petrologic studies of garnet zoning, the composition profiles are only measured on the largest garnets, the reason being that these should contain the most information about the P–T path. So it is possible that the effect may have been overlooked in many studies.

The shapes of X_{sps} profiles shown in Figs. 5 and 6 provide constraints on the rate limiting step in garnet growth. As mentioned above, the computed profiles for the Stefan's interface model are considerably flatter than what has been reported for progressively nucleated garnet (e.g. Chernoff and Carlson, 1997). Examples of peaked Mn zoning in the center of garnet cores have, in fact, been observed in garnets from the Connecticut Valley Synclinorium, central Vermont (Fig. 8), similar to constant radius or constant flux models, and suggests that interface control may be rate limiting for the growth of these garnets. Similarly peaked Mn zoning profiles in garnet have also been reported by George and Gaidies (2017 – their Fig. 12)

3.2. Garnet growth and the approach to equilibrium

The OS models presented above for garnet growth were calculated for isothermal, isobaric growth as a limiting case. The garnet producing reaction was allowed to run to completion, which occurred when chlorite (a necessary reactant) was depleted. However, the question remains as to how close is the approach to equilibrium at the point where garnet stopped growing.

This question was addressed for a sample from the Gile Mountain Formation in eastern Vermont (sample TM-626), which was also examined by Spear et al. (2014). Fig. 9 displays two pseudosections for this sample, one calculated for the whole rock bulk composition (Fig. 9a) and the other for the bulk composition with garnet subtracted (Fig. 9b; Table 1). Both diagrams were calculated assuming equilibrium in the MnNCKFMASH system with only the phases quartz, muscovite, fluid, plagioclase, chlorite, biotite, and garnet considered for simplicity. The results of quartz inclusion in garnet (QuiG) barometry, as discussed by Spear et al. (2014), suggested that garnet nucleated well above the nominal isograd reaction. The intersection of garnet core isopleths assuming equilibrium (red star, Fig. 9a) would imply that garnet nucleated at approximately 8 kbar, 575 °C, the latter a few tens of degrees above the equilibrium garnet isograd. However, the QuiG barometry, which records conditions of quartz inclusion entrapment in garnet, suggests that the conditions of garnet nucleation were at least 675 °C, 10.5 kbar, and possibly as high as 690 °C, 13.7 kbar (yellow stars, Fig. 9a).

Two additional sets of calculations were done using the bulk compositions from Fig. 9 in which garnet was not permitted to be a part of the stable assemblage, but in which the composition of garnet was calculated at each P–T point from the OS model (Fig. 1). The isopleth for the Fe/(Fe + Mg) for the garnet core and rim are plotted in Fig. 9a and b (green lines). The intersection of these isopleths with the QuiG barometry are interpreted as reflecting the conditions of garnet nucleation (Fig. 9a, yellow stars) and final growth (Fig. 9b, green stars). If this interpretation is valid, then it is apparent that the P–T conditions changed very little from garnet nucleation to final growth: that is, in this sample garnet grew nearly isothermally and isobarically. Furthermore, examination of the isopleths for the garnet rim (red lines in Fig. 9b) do not intersect closely, and would imply that the garnet rim P–T conditions were at lower temperature than the core, which seems unrealistic. The affinity required for garnet nucleation from these

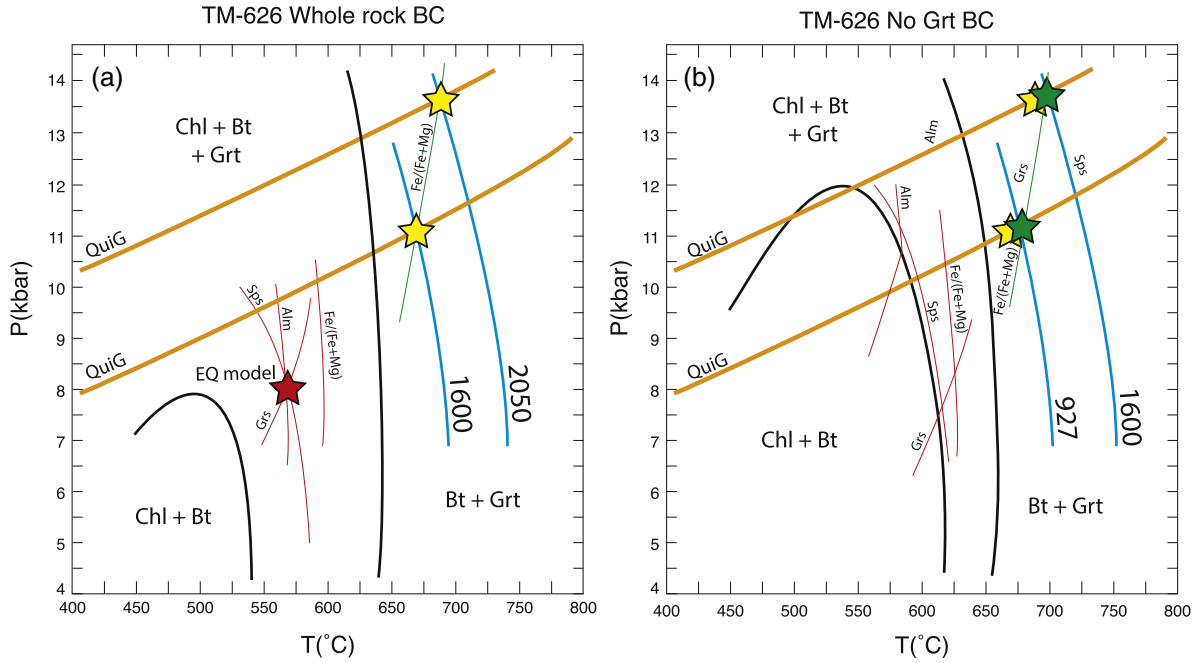

Fig. 9. P-T diagrams showing the results of calculations for sample TM-626. (a) Simplified equilibrium MAD for the whole rock bulk composition. (b) Simplified equilibrium MAD for the bulk composition with garnet removed. Black lines are MAD assemblage boundaries (all assemblages also include quartz + muscovite + plagioclase + fluid). Orange lines show the range of inferred P-T conditions of quartz inclusion entrapment in garnet from QuiG barometry. Thin red lines are isopleths of garnet composition for the core (a) and rim (b) from the EQ model. Thin green lines are isopleth of Fe/(Fe + Mg) in garnet for the core (a) and rim (b) from the OS model. Red and yellow stars in (a) are the inferred conditions of garnet nucleation from the EQ and OS models. Green stars in (b) are the inferred conditions for the garnet rim from the OS model. Blue lines are contours of affinity in J/mol O. (For interpretation of the references to colour in this figure legend, the reader is referred to the web version of this article.)

calculations is either 1600 or 2050 J/mol O, depending on which QuiG isopleth is used, and the affinity at the end of garnet growth is 927 or 1600 J/mol O, reflecting a decrease in affinity from nucleation to growth of 450 to 673 J/mol O. The implication is that the rock did not achieve equilibrium even at the end of the growth of garnet.

4. Discussion

The nucleation of garnet and other porphyroblasts requires a degree of overstepping of the equilibrium isograd reaction. Unfortunately, the amount of overstepping for initial nucleation is difficult to constrain, as revealed by the wide range of estimates from the above studies, and there are no general theoretical criteria that have been developed to handle the complexity of real rocks. It is likely that the amount of overstepping varies based on the bulk composition, preexisting mineralogy, and strain history. Nevertheless, the observational data available at this time suggests affinities of several hundred to a few thousands of joules/mol oxygen are required to nucleate garnet, which corresponds to several tens of degrees or several kilobars of overstepping. In addition, the analysis presented above for sample TM-626 suggests that the sample may never have reached an equilibrated state, even near the peak metamorphic conditions, because the affinity for reaction never reaches zero.

It would appear, therefore, that the traditional approach of assuming (explicitly or tacitly) that garnet growth occurs at near-equilibrium conditions needs reexamination. Some studies where isopleths from central-sectioned garnets intersect near the garnet-in isograd have been taken as evidence for near-equilibrium growth, but it has been demonstrated by Spear et al. (2014) that such a near-coincidence with the garnet isograd is expected when garnet nucleates after significant overstepping. Additionally, if garnet nucleation requires affinities of several hundred joules to nucleate, then the nucleation and subsequent growth of this initial garnet will deplete the reservoir of affinity needed to nucleate additional garnets. It is not sufficient, as has been assumed by Ketcham and Carlson (2012) and Kelly et al. (2013a, 2013b), to decrease the affinity for nucleation to only restricted regions in the rocks that suffer Al depletion because all of the cations incorporated into garnet (Mn, Ca, Fe, Mg) will be depleted by initial garnet growth, which will lower the affinity for nucleation throughout the entire rock (Fig. 3). The well-demonstrated fact of progressive nucleation in many rocks (e.g. Chernoff and Carlson, 1997; Spear and Daniel, 1998) thus negates the possibility that garnet growth occurs at near-equilibrium conditions, unless the affinity required for progressive nucleation decreased significantly after the initial garnet nucleated, which seems highly unlikely.

Thus it may be that most previous studies (the author's included) that use observed garnet zoning with thermodynamic calculations assuming equilibrium conditions need to be reevaluated. These include not only studies that use garnet zoning and inverse modeling such as with the Gibbs method (e.g. Spear and Selverstone, 1983) or forward models that use pseudosections (e.g. Gaidies et al., 2011), but also methods that use classical thermobarometry with inclusion suites in garnet (e.g. St-Onge, 1987).

As the kinetics of mineral nucleation and growth and the processes that operate on grain boundaries on the nano scale become better understood, it is likely that new methods will emerge that will permit better elucidation of the evolution of a metamorphic rock than is currently possible. For example, the model presented here in which the composition of garnet growing out of equilibrium is assumed to be the composition that provides the largest decrease in free energy indicates a direction for future research. Specifically, it has been shown that this approach provides a means of calculating conditions of both garnet nucleation and final growth, so it should be possible to invert the process and calculate the changes in pressure and temperature necessary to grow a garnet with an observed zoning pattern, similar to the approach used to create Fig. 9. Such an approach may open new avenues of investigation of rocks undergoing active metamorphism.

Acknowledgments

This work was supported by a grant from the National Science Foundation (1447468 to F. S. Spear and J. B. Thomas) and the Edward P. Hamilton Distinguished Scientist endowed chair. The author wishes to thank Oliver Wolfe for assistance in the collection of garnet X-ray maps and David Pattison for stimulating discussions. Thorough and thoughtful reviews by D. Waters and P. Robinson are gratefully acknowledged.

References

Carlson, W.D., 1989. The significance of intergranular diffusion to the mechanisms and kinetics of porphyroblast crystallization. Contrib. Mineral. Petrol. 103, 1–24.
Carlson, W.D., 1991. Competitive diffusion-controlled growth of porphyroblasts. Mineral. Mag. 55, 317–330.
Castro, A., Spear, F.S., 2016. Reaction overstepping and reevaluation of the peak P-T conditions of the Blueschist unit Sifnos, Greece: implications for the Cyclades subduction zone. Int. Geol. Rev. 59, 548–562.
Chakraborty, S., Ganguly, J., 1992. Cation diffusion in aluminosilicate garnets - experimental determination in spessartine-almandine diffusion couples, evaluation of effective binary diffusion coefficients, and applications. Contrib. Mineral. Petrol. 111, 74–86.
Chernoff, C.B., Carlson, W.D., 1997. Disequilibrium for ca during growth of pelitic garnet. J. Metamorph. Geol. 15, 421–438.
Denison, C., Carlson, W.D., 1997. Three-dimensional quantitative textural analysis of metamorphic rocks using high-resolution computed X-ray tomography: part II. Application to natural samples. J. Metamorph. Geol. 15, 45–57.
Frost, B.R., Tracy, R.J., 1991. P-T paths from zoned garnets: some minimum criteria. Am. J. Sci. 291, 917–939.
Gaidies, F., De Capitani, C., Abart, R., 2008. THERIA_G: a software program to numerically model prograde garnet growth. Contrib. Mineral. Petrol. 155, 657–671.
Gaidies, F., Pattison, D.R.M., de Capitani, C., 2011. Toward a quantitative model of metamorphic nucleation and growth. Contrib. Mineral. Petrol. 162 (5), 975–993.
George, F.R., Gaidies, F., 2017. Characterisation of a garnet population from the Sikkim Himalaya: insights into the rates and mechanisms of porphyroblast crystallisation. Contrib. Mineral. Petrol. 172.
Glicksman, M.E., 2000. Diffusion in Solids. John Wiley & Sons, Inc., New York (472 pp).
Hollister, L.S., 1966. Garnet zoning: an interpretation based on the Rayleigh fractionation model. Science 154, 1647–1651.
Hollister, L.S., 1969. Contact metamorphism in the Kwoiek Area of British Columbia: an end member of the metamorphic process. Geol. Soc. Am. Bull. 80, 2465–2494.
Kelly, E.D., Carlson, W.D., Ketcham, R.A., 2013a. Magnitudes of departures from equilibrium during regional metamorphism of porphyroblastic rocks. J. Metamorph. Geol. 31, 981–1002.
Kelly, E.D., Carlson, W.D., Ketcham, R.A., 2013b. Crystallization kinetics during regional metamorphism of porphyroblastic rocks. J. Metamorph. Geol. 31, 963–979.
Ketcham, R.A., Carlson, W.D., 2012. Numerical simulation of diffusion-controlled nucleation and growth of porphyroblasts. J. Metamorph. Geol. 30, 489–512.
Kirkpatrick, R.J., 1975. Crystal growth from the melt: a review. Am. Mineral. 60, 798–814.
Kretz, R., 1974. Some models for the rate of crystallization of garnet in metamorphic rocks. Lithos 7, 123–131.
Pattison, D.R.M., Tinkham, D.K., 2009. Interplay between equilibrium and kinetics in prograde metamorphism of pelites: an example from the Nelson aureole, British Columbia. J. Metamorph. Geol. 27, 249–279.
Pattison, D.R.M., de Capitani, C., Gaidies, F., 2011. Petrological consequences of variations in metamorphic reaction affinity. J. Metamorph. Geol. 29 (9), 953–977.
Spear, F.S., Daniel, C.G., 1998. 3-Dimensional imaging of garnet porphyroblast sizes and chemical zoning. Nucleation and growth history in the garnet zone. Geol. Mater. Res. 1 (1), 1–43.
Spear, F.S., Daniel, C.G., 2001. Diffusion control of garnet growth, Harpswell Neck, Maine, USA. J. Metamorph. Geol. 19, 179–195.
Spear, F.S., Pattison, D.R.M., 2017. The implications of overstepping for metamorphic assemblage diagrams (MADs). Chem. Geol. 457, 38–46.
Spear, F.S., Pyle, J.M., 2010. Theoretical modeling of monazite growth in a low-Ca metapelite. Chem. Geol. 273 (1–2), 111–119.
Spear, F.S., Selverstone, J., 1983. Quantitative P-T paths from zoned minerals: theory and tectonic applications. Contrib. Mineral. Petrol. 83, 348–357.
Spear, F.S., Kohn, M.J., Florence, F., Menard, T., 1990. A model for garnet and plagioclase growth in pelitic schists: implications for thermobarometry and P-T path determinations. J. Metamorph. Geol. 8, 683–696.
Spear, F.S., Thomas, J.B., Hallett, B.W., 2014. Overstepping the garnet isograd: a comparison of QuiG barometry and thermodynamic modeling. Contrib. Mineral. Petrol. 168 (3), 1–15.
St-Onge, M.R., 1987. Zoned poikiloblastic garnets: P-T paths and syn-metamorphic uplift through 30 km of structural depth, Wopmay Orogen, Canada. J. Petrol. 28, 1–22.
Symmes, G.H., Ferry, J.M., 1992. The effect of whole-rock MnO content on the stability of garnet in pelitic schists during metamorphism. J. Metamorph. Geol. 10 (MAR), 221–237.
Thompson, C.V., Spaepen, F., 1983. Homogeneous crystal nucleation in binary metallic melts. Acta Metall. 31, 2021–2027.
Volmer, M., Marder, M., 1931. Zur theorie der linearen kristallisationsgeschwindigkeit. Z. Phys. Chem. 154, 97–112.
Waters, D.J., Lovegrove, D.P., 2002. Assessing the extent of disequilibrium and overstepping of prograde metamorphic reactions in metapelites from the Bushveld Complex aureole, South Africa. J. Metamorph. Geol. 20 (1), 135–149.
Wilbur, D.E., Ague, J.J., 2006. Chemical disequilibrium during garnet growth: Monte Carlo simulations of natural crystal morphologies. Geology 34 (8), 689–692.